Integrated geological and petrophysical studies for reservoir characterization of the Jurassic Safa formation, Syrah Field, Shushan Basin, North Western Desert, Egypt

Elsawy, M.S[1], Abdelfatah, M.A.[2], Abdeldayem, A.L.[3], and Abdelraheem, S.H.[3]

[1]Khalda Petroleum Company, Cairo, Egypt
[2]Geology Department, Faculty of Science, Cairo University, Egypt
[3]Geology Department, Faculty of Science, Tanta University, Egypt
Mohammed.elsawy@khalda-eg.com

Abstract: This research work is dedicated to the establishment of an efficient workflow to evaluate petroleum reservoir potentials. This has been achieved through detailed petrographical and petrophysical studies of the Jurassic Safa Formation in the Syrah Field (defined in 4 studied wells, Syrah – 1X, Syrah – 5X, Syrah – 6Xst and Syrah – 8X), northern Western Desert, Egypt. Such workflow has enabled the detection of structural pattern and sedimentary structures and depiction of depositional environment. Different microfacies of the studied intervals have been identified petrographically and used as a reference to integrate gamma ray, density and neutron logs to extract continuous accurate lithological column. Spectral gamma ray logs, available from the used 4 wells, were used to determine the clay type present in the reservoir interval. Evaluation of the Safa Formation could be accomplished through the analysis of lithofacies types and determination of the different reservoir parameters characterizing the pay zone through the use of available well log data where promising locations for further development and exploration could be spotted. Petrophysical data analysis vertically via the Litho- Saturation cross-plots and laterally through the iso-parametric maps helped in defining the lateral variation of petrophysical parameters, reservoir thickness and locating suitable places for drilling new productive wells. It also showed that the Syrah field is characterized by good reservoir parameters. Study of reservoir pressure was used to determine reservoir fluid type and check the connectivity of hydrocarbon sand-bearing zones. Based on the obtained results, it can be stated that the Syrah field may attain commercial hydrocarbon accumulation in Safa Formation, and there is a good opportunity to drill more development and exploratory wells to enhance its productivity. Integration of different results helped in the establishment of a depositional model for both Upper and Lower Safa reservoirs. Sand channel directions and quality were also determined.

[Elsawy, M.S, Abdelfatah, M.A., Abdeldayem, A.L., and Abdelraheem, S.H. **Integrated geological and petrophysical studies for reservoir characterization of the Jurassic Safa formation, Syrah Field, Shushan Basin, North Western Desert, Egypt.** *Nat Sci* 2018;16(8):53-65]. ISSN 1545-0740 (print); ISSN 2375-7167 (online). http://www.sciencepub.net/nature. 7. doi:10.7537/marsnsj160818.07.

Keywords: Integrated geological; petrophysical; reservoir; characterization; Jurassic Safa formation; Syrah Field; Shushan Basin; North Western Desert; Egypt

1. Introduction

The Western Desert of Egypt still has a significant hydrocarbon potential as recent oil and gas discoveries have suggested (Dolson et al., 2001). Perhaps 90 % of undiscovered oil reserves and 80% of undiscovered gas reserves in Egypt are located in the Western Desert (Zein El-Din et al., 2001). The Syrah field that forms the scope of this study lies in the Shushan Basin, north Western Desert, Egypt (Figure 1). It is bounded by latitudes 30° 39' 10" – 30° 42' 8" N and longitudes 26° 40' 23"- 26° 44' 12" E.

2. Geological Setting

The northern part of the Western Desert comprises a number of sedimentary basins that received a thick succession of Mesozoic sediments. The general stratigraphic section in the northern Western Desert ranges in age from Paleozoic to Cenozoic (Neogene) as summarized in figure 2. The post- Paleozoic succession in this area comprises four sedimentary cycles of Lower to Upper Jurassic, Lower Cretaceous, Upper Cretaceous, and Eocene to Miocene (Sultan and Halim, 1988).

The Shushan Basin, which is the largest of the coastal basins, is a half-graben system with a maximum thickness of 7.5 km of Jurassic, Cretaceous, and Paleogene sediments (El Shazly, 1977; Hantar, 1990). This basin witnessed Jurassic and Early Cretaceous extension that was followed by Late Cretaceous early Tertiary inversion (El Awdan et al., 2002).

The Safa Formation is divided into lower and upper parts by the Kabrit member that is characterized by predominance of limestones. The Lower Safa member is composed of shale, siltstone, sandstone and Limestone streaks, it is underlies the Kabrit Member, while the Upper Safa Member overlies the Kabrit Member.

The Upper Safa Member is composed of siltstones, sandstone and shale with minor of limestone streaks.

3. Results and Discussions

3.1. Petrographic examination

The petrographic description of nineteen drill cutting samples, selected based on upnormal log phenomena, helped in the identification of 16 microfacies types (7 sandstones, one carbonates, two mudstones and 6 metamorphic) that comprise quartz arenite, dolomitic / ferroan dolomitic quartz arenite, kaolinitic quartz arenite, sideritic quartz arenite, chloritic quartz arenite, quartz wacke, kaolinitic quartz wacke, fe-dolomitic mudstone, mudstone, crystalline dolomite, sideritie, slate, phyllite, quartz-mica schist, meta- basalt, and Mylonite (Figures 2-7) (**Khalda Petroleum Company Internal Report, 2014**).

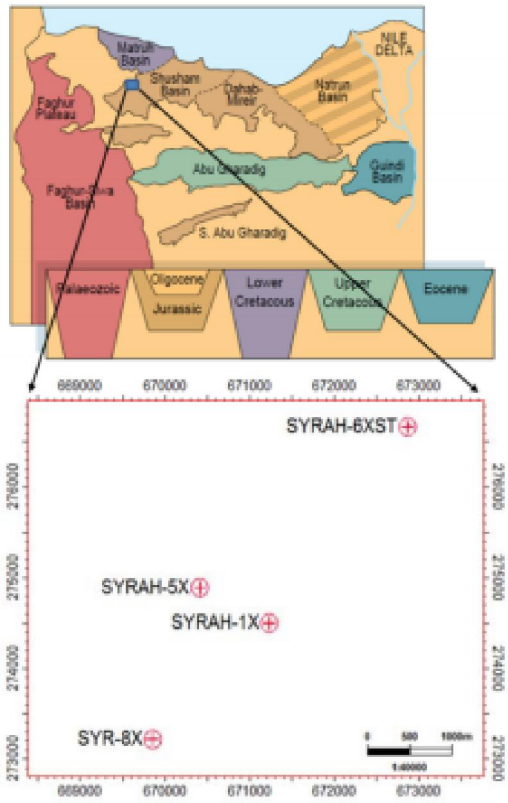

Figure 1: Location map of the study area showing the location of the used wells in SYRAH field, North Western Desert, Egypt.

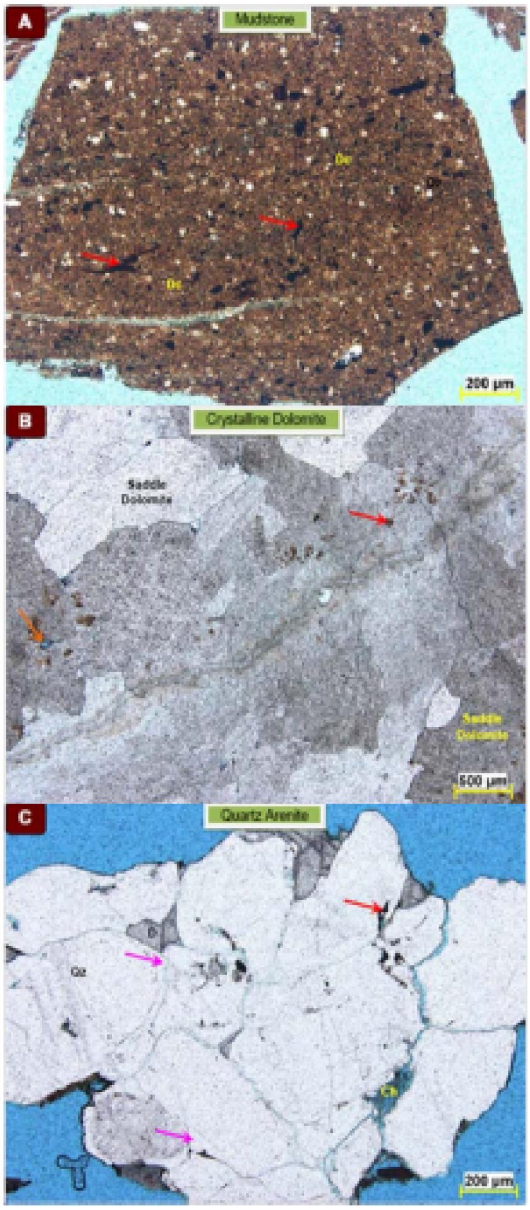

Figure 2: Ditch sample thin section at depth 13600 ft, Upper Safa, SYRAH – 1X.

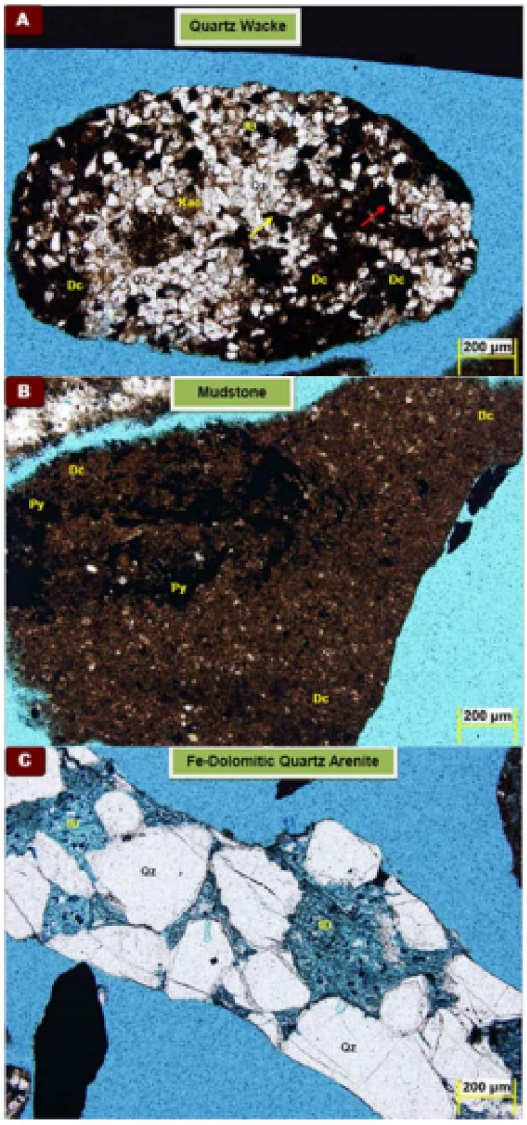

Figure 3: Ditch sample thin section at depth 13680 ft Upper Safa, SYRAH – 5X

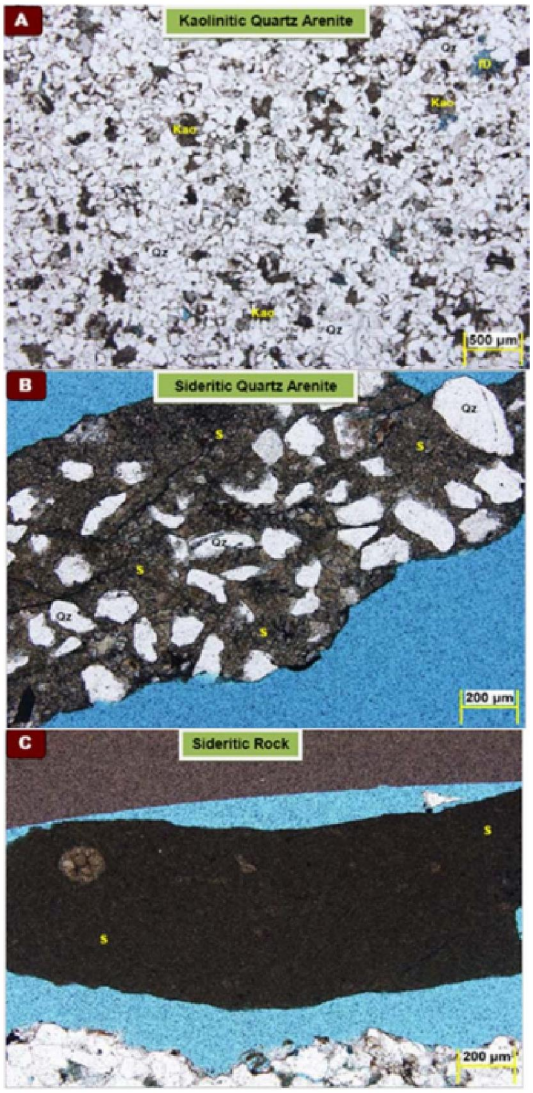

Figure 4: Ditch sample thin section at depth 13850 ft Upper Safa, SYRAH – 5X

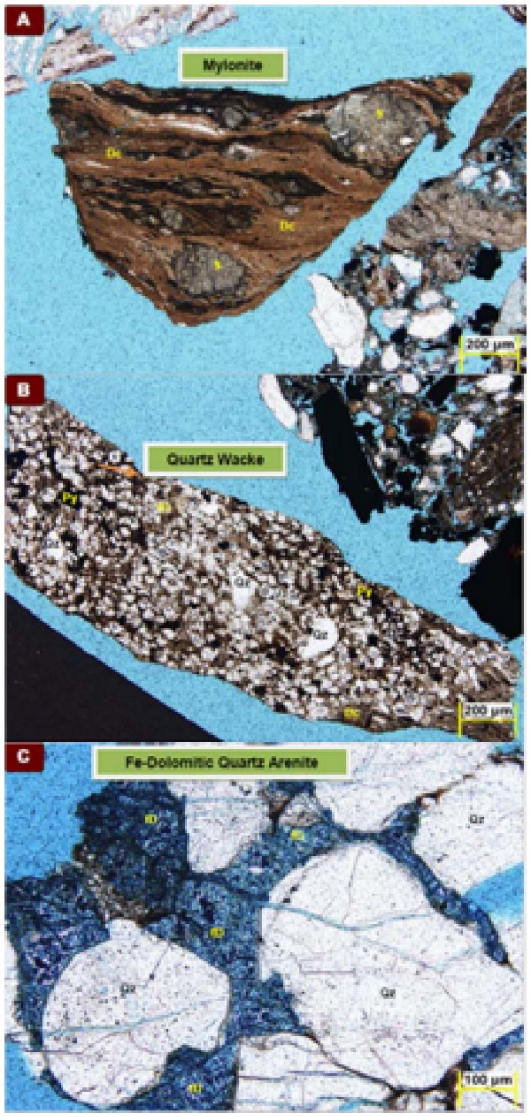

Figure 5: Ditch sample thin section at depth 13850 ft Upper Safa, SYRAH – 6Xst

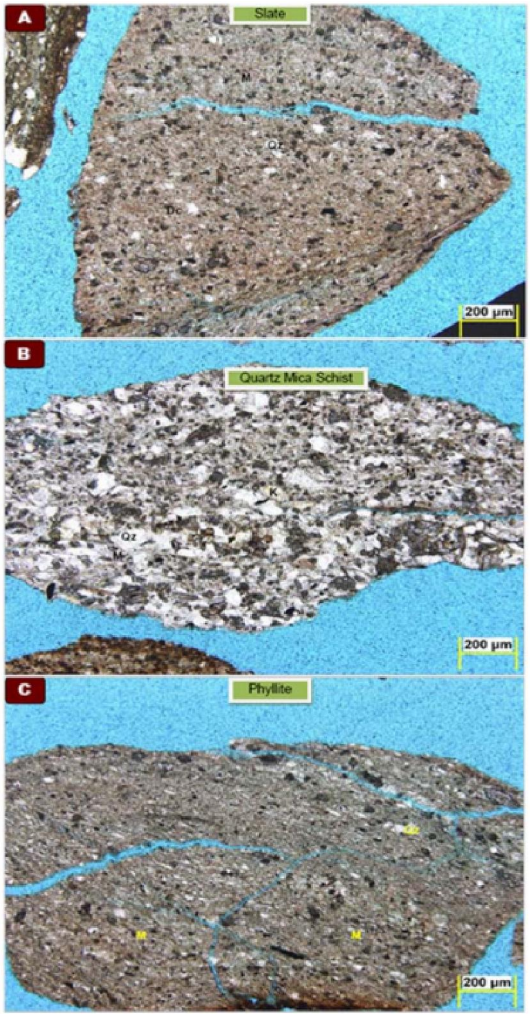

Figure 6: Ditch sample thin section at depth 13910 ft, Lower Safa, SYRAH – 1X

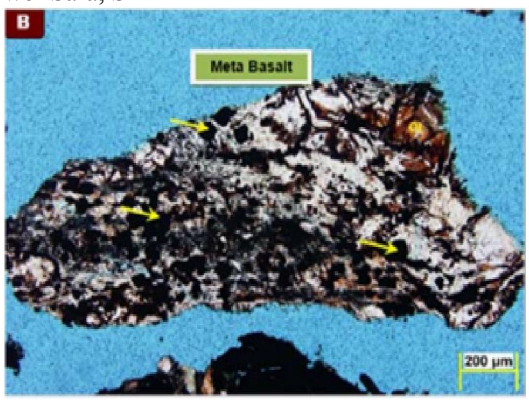

Figure 7: Ditch sample thin section at depth 13900 ft Upper Safa, SYRAH – 6Xst

These microfacies have been used as a reference to the integration of gamma ray, density and neutron logs to extract continuous accurate lithological column as summarized below:

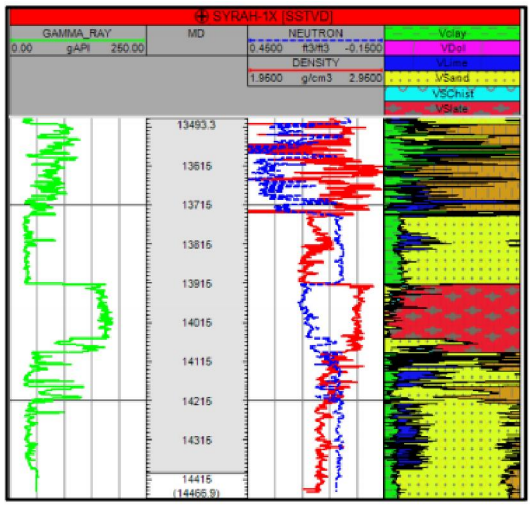

Figure 8: Lithological interpretation of Syrah – 1X

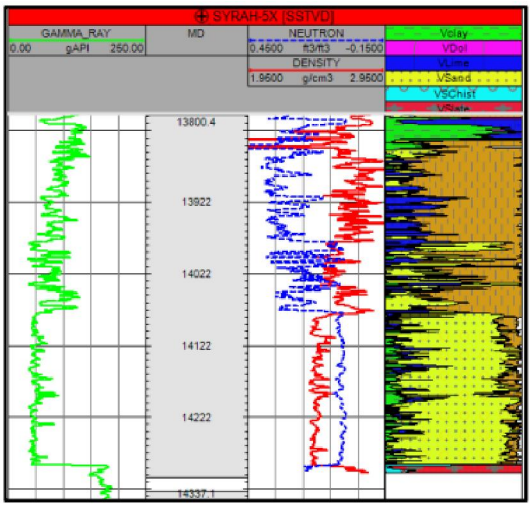

Figure 9: Lithological interpretation of Syrah – 5X

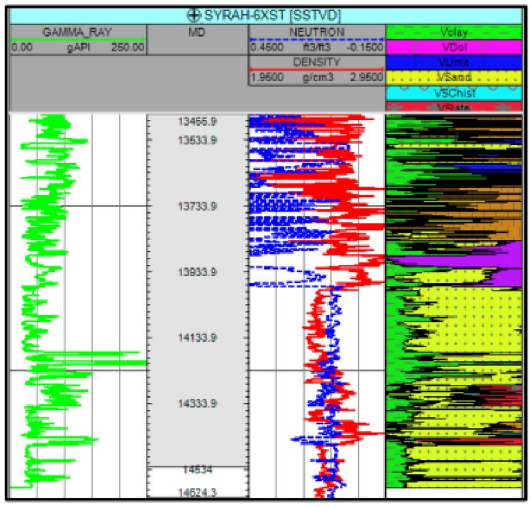

Figure 10: Lithological interpretation of Syrah – 6Xst

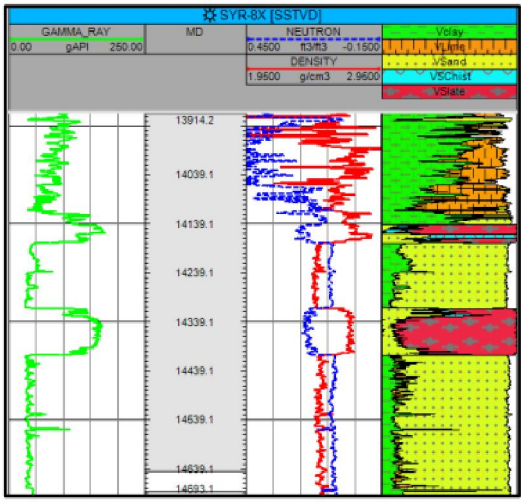

Figure 11: Lithological interpretation of Syrah – 8X

- Most of the section is composed of intercalations of clastic rocks except for some zones with metamorphic rocks that could not be identified directly from logs and are detailed below as detected in the four studied wells:

- Syrah – 1X, 94 % slate, 4 % quartz mica schist and 2 % phyllite, detected at depth from 13917 to 14091ft (Figure 8).
- Syrah – 5X, 90 % slate and 10 % quartz mica schist occupying the depth from 14288 to 14510 ft (Figure 9).
- Syrah – 6XST has two zones of metamorphic rocks; the first from 13875 to 13925 ft and consists of metabasalt and, the second from 14280 to 14340 ft and consists of 35 % slate, 10% phyllite and 55 % quartz mica schist (Figure 10).

Syrah – 8X has two zones of metamorphic rocks, the first from 14139 to 14177 ft with 70 % slate, 20 % phyllite and 10 % quartz mica schist, and the second from 14311 to 14407 ft with 95 % slate, 3 % quartz mica schist and 2 % phyllite (Figure 11).

3.2 Formation Evaluation

3.2.1 Types of clay minerals

Determination of clay minerals content is limited to five typical minerals which are significant for the oil industry: chlorite, glauconite, illite, kaolinite and smectite **(Schlumberger, 1985)**.

Information about clay mineral types in a studied formation is used for example, for selecting a proper drilling fluid, because application of inappropriate fluid may cause swelling of clay minerals.

To study clay mineral types in the study area, the distribution of thorium and uranium has been followed. Th-K cross plots were constructed to show clay mineral types in the study wells. Figures (12 and 13) show the presence of different clay types in the Upper Safa member in Syrah – 1X. There are scattered

points around mixed layered with some points around illite, mica and glauconite. Figure (14) shows the presence of different clay types in the Lower Safa Member in Syrah – 1X. There is a cluster around illite with some points around glauconite, mixed layered and few points around mica. Figures (15 and 17) are histograms of the percentage of each clay mineral type within the upper Safa and lower Safa members in Syrah – 1X well.

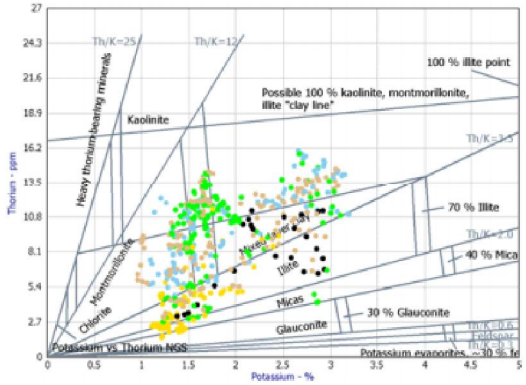

Figure 12: Clay mineral types based on the Th/K cross plot for Upper Safa, Syrah-1X well.

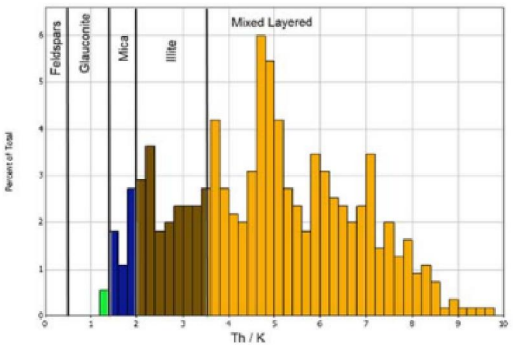

Figure 13: Clay minerals based on histograms of the Th/K ratio for Upper Safa, Syrah – 1X well

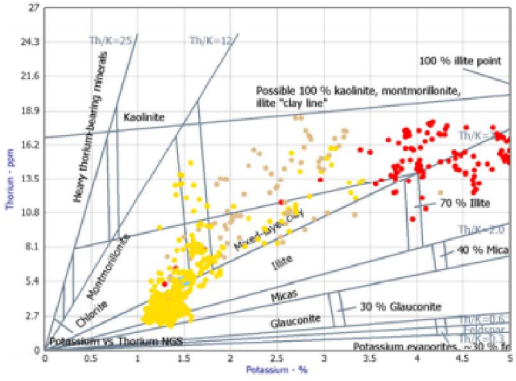

Figure 14: Clay mineral types based on the Th/K cross plot for lower Safa, Syrah-1X well.

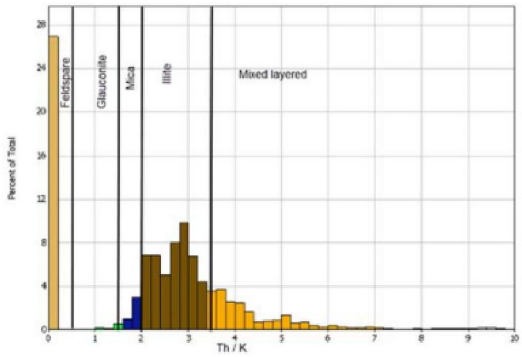

Figure 15: Clay minerals based on histograms of the Th/K ratio for Lower Safa, Syrah – 1X well.

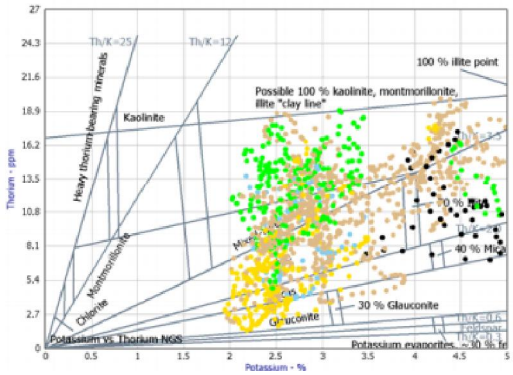

Figure 16: Clay mineral types based on the Th/K cross plot for Upper Safa, Syrah-5X well.

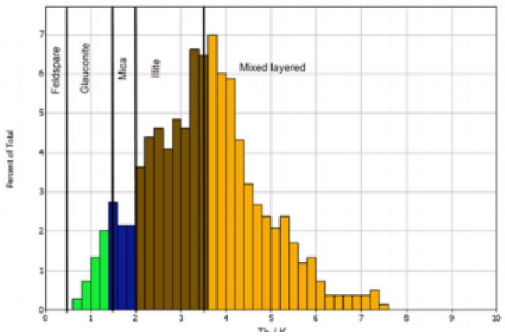

Figure 17: Clay minerals based on histograms of the Th/K ratio for Upper Safa, Syrah – 5X well.

Figure (16) shows the presence of different clay types in the Upper Safa member in Syrah – 5X well. There are a scattered points around illite, mixed layered, and few points around mica, glauconite and feldspars. Figure (18) shows the presence of different clay types in the lower Safa member in Syrah – 5X well. There are two clusters the first one around Illite and second around glauconite. There are also few scattered points around mixed layered and mica and minor points around feldspars. Figures (17 and 19) are histograms showing the percentage of each clay type

within the upper Safa and lower Safa members in Syrah – 5X well.

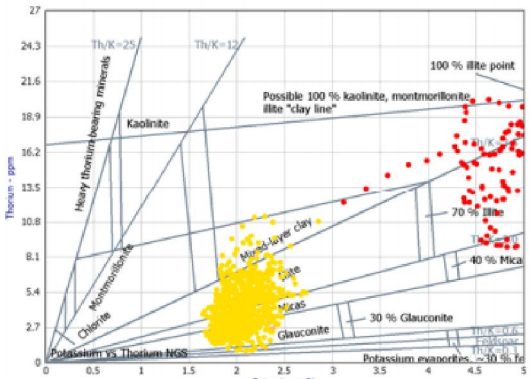

Figure 18: Clay mineral types based on the Th/K cross plot for lower Safa, Syrah-5X well.

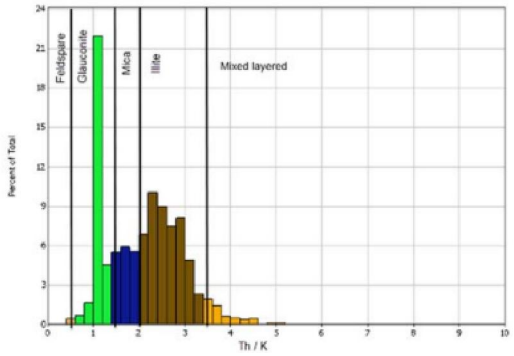

Figure 19: Clay minerals based on histograms of the Th/K ratio for Lower Safa, Syrah – 5X well.

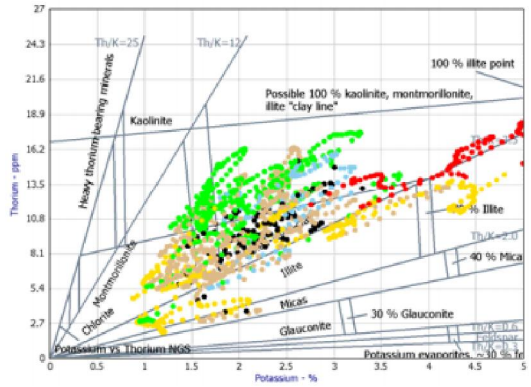

Figure 20: Clay mineral types based on the Th/K cross plot for upper Safa, Syrah-6Xst well.

Figure (20 and 21) shows scattered points around illite, mixed layered, and few points around mica, glauconite and feldspars. Figure (23) shows the presence of different clay types in the Lower Safa member in Syrah – 6Xst well. There is a cluster around mixed layered, and few scattered points around illite. Figure (22 and 24): showing the histogram percentage of each clay type within upper and lower Safa members in Syrah – 6Xst.

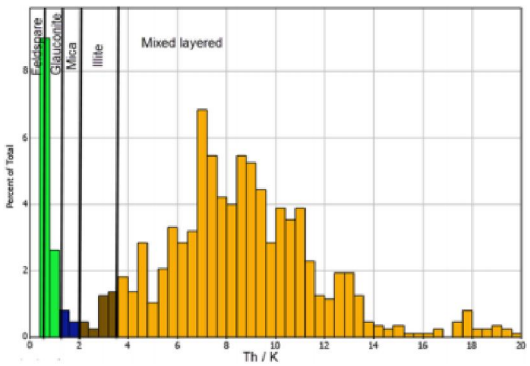

Figure 21: Clay minerals based on histograms of the Th/K ratio for upper Safa, Syrah – 6Xst well.

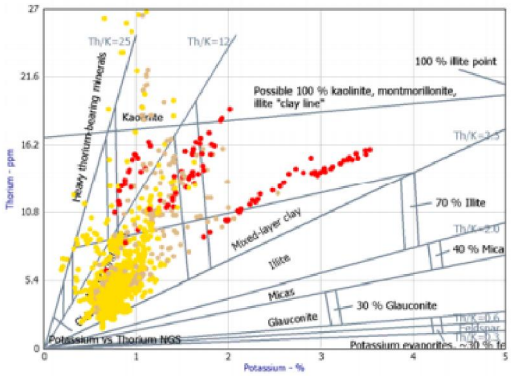

Figure 22: Clay mineral types based on the Th/K cross plot for lower Safa, Syrah-6Xst well.

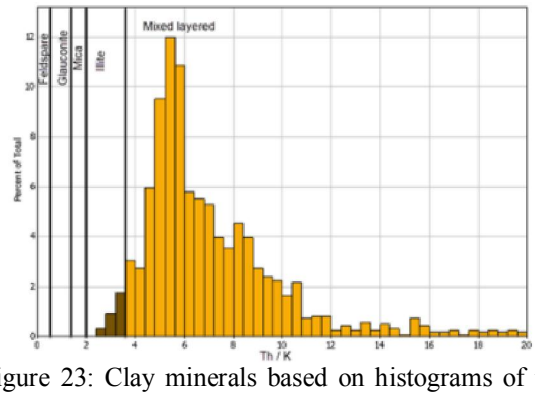

Figure 23: Clay minerals based on histograms of the Th/K ratio for lower Safa, Syrah – 6Xst well.

Figure (24) shows the presence of different clay types in the Upper Safa member in Syrah – 8X well. There are scattered points around mixed layered, illite, and few points around mica. Figure (26) shows the presence of different clay types in the lower Safa member in Syrah – 8X well. There are two clusters; the first is around illite and the second is around mixed

layered. There are also few points around mica. Figures (25 and 27) show the histogram percentage of each clay type within the Upper and Lower Safa members in Syrah – 8X well, as shown in the cross plots.

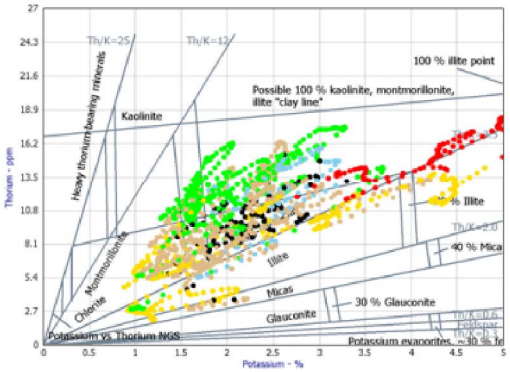

Figure 24: Clay mineral types based on the Th/K cross plot for upper Safa, Syrah-8X well.

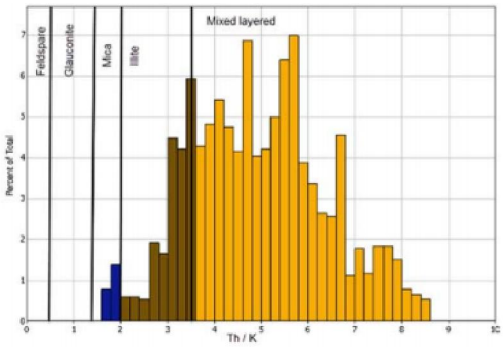

Figure 25: Clay minerals based on histograms of the Th/K ratio for upper Safa, Syrah – 8X well.

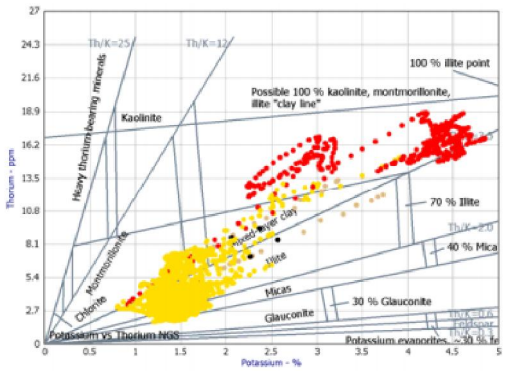

Figure 26: Clay mineral types based on the Th/K cross plot for lower Safa, Syrah-8X well.

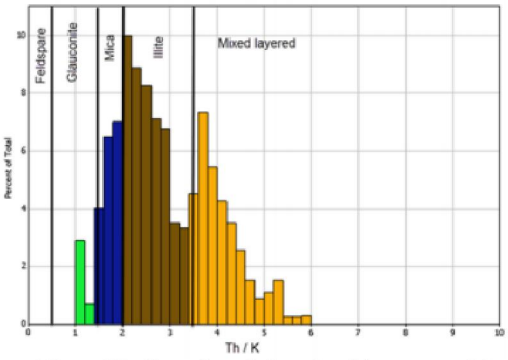

Figure 27: Clay minerals based on histograms of the Th/K ratio for lower Safa, Syrah – 8X well.

Figure 27: Clay minerals based on histograms of the Th/K ratio for lower Safa, Syrah – 8X well.

3.2.2 Petrophysical Evaluation

Conventional petrophysical analysis was performed for the Safa Formation in the four studied wells to determine the petrophysical parameters through reservoir interval to enable the construction of petrophysical parameter maps to be used to establish the spatial distribution of the petrophysical parameters.

Hydrocarbon potentialities resulting from the above mentioned petrophysical parameters for the 4 wells are presented in the form of a set of shale volume, porosity and water saturation maps for Safa Formation. It demonstrated that the Upper Safa has high oil potentiality in all the studied wells while Lower Safa has a good gas potentiality in only three wells (Syrah – 1X, Syrah – 5X and Syrah – 6Xst).

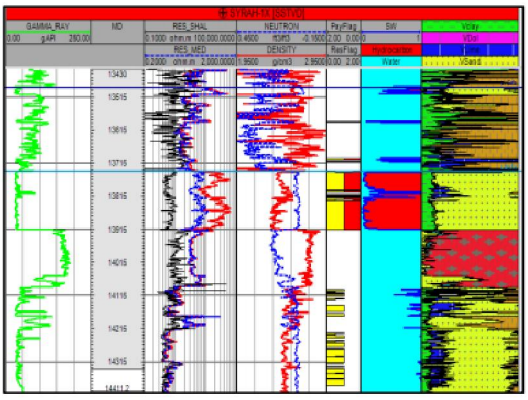

Figure 28: Vertical distribution of Petrophysical and lithology results of Safa in Syrah-1X.

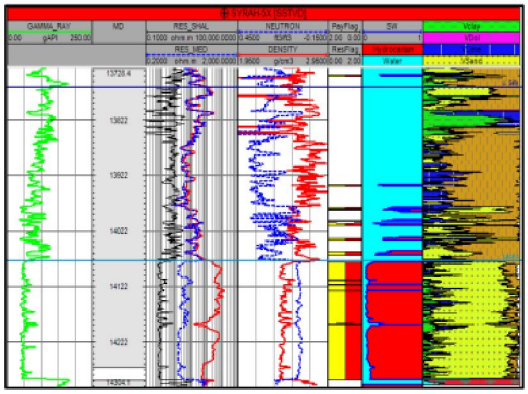

Figure 29: Vertical distribution of Petrophysical and lithology results of Safa formation in Syrah-5X.

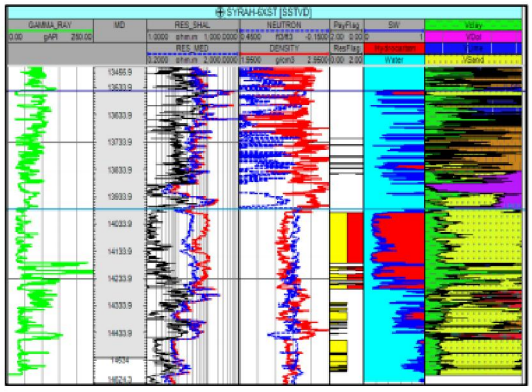

Figure 30: Vertical distribution of Petrophysical and lithology results of Lower Safa in Syrah-6Xst.

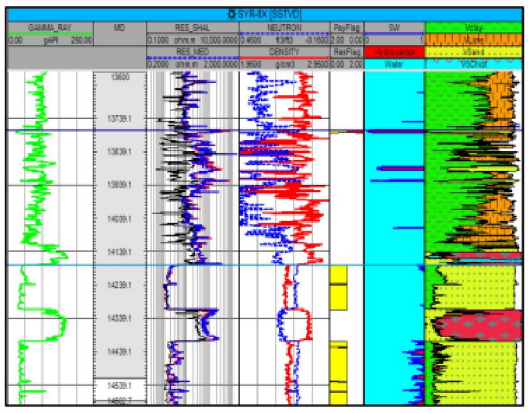

Figure 31: Vertical distribution of Petrophysical and lithology results of Lower Safa in Syrah-8X.

3.2.2 Reservoir Pressure Measurement

The analysis of pressure data of Lower Safa reservoir in Syrah - 1X well reflect gas gradient of 0.11 psi/ft in upper sandstone and water gradient of 0.5 psi/ft, as shown in figure (32). In Syrah - 5X well it reflects gas gradient of 0.1 psi/ft (Figure 33) while in Syrah - 6Xst well it reflects gas gradient of 0.11 psi/ft in Upper sandstone zone and water gradient of 0.47 psi/ft in the lowest one (Figure 34). In Syrah - 8X well it reflects water for both the upper sandstone zone of 0.46 psi/ft and the lowest sandstone zone of 0.5 psi/ft, (Figure 35).

Pressure values range from 6240 to 6280 psi in Syrah – 1X, Syrah – 5X and Syrah – 6Xst, indicating connectivity and 6950 psi in Syrah – 8X reflecting isolation in pressure.

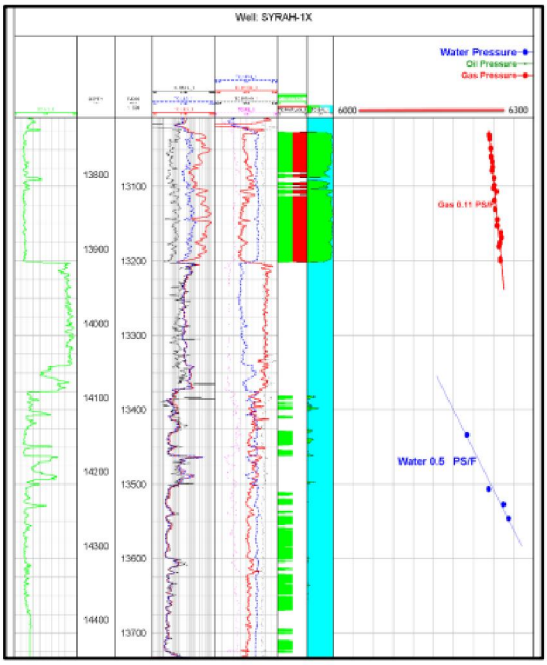

Figure 32: Analysis of Lower Safa pressure data in Syrah -1X well

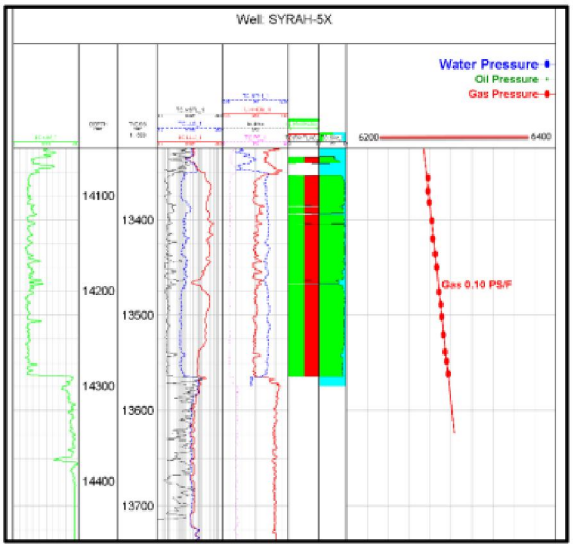

Figure 33: Analysis of Lower Safa pressure data in Syrah -5X well

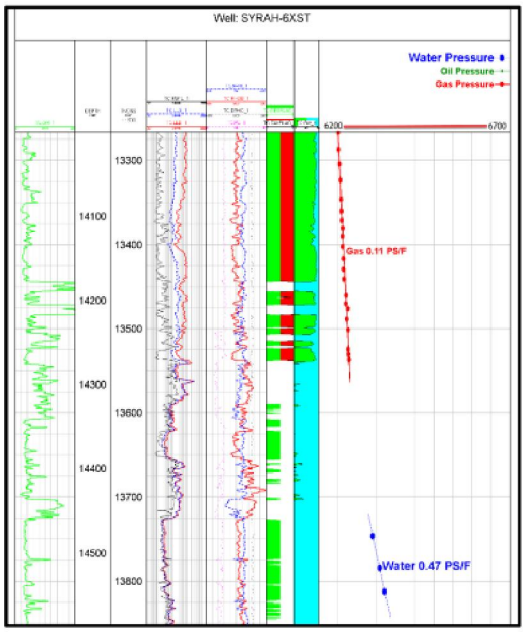

Figure 34: Analysis of Lower Safa pressure data in Syrah -6Xst well

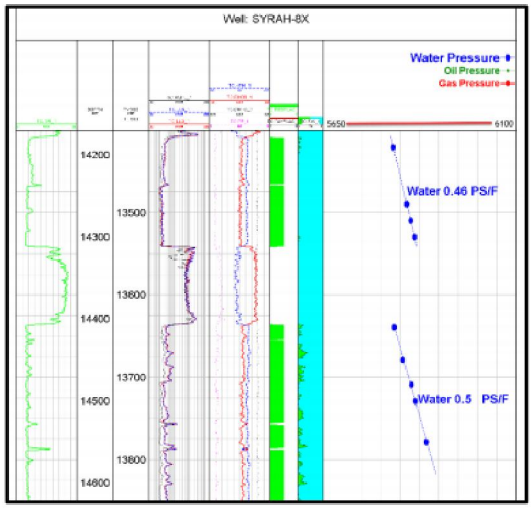

Figure 35: Analysis of Lower Safa pressure data in Syrah -8X well

3.2.3 Formation mapping

After calculating the values of the log- derived parameters for Upper and Lower Safa reservoirs, we need to average and map these parameters to represent their general distribution throughout the Syrah Field.

3.2.3.1 Upper Safa Reservoir maps

The total thickness distribution map for Upper Safa reservoir in Syrah field (Figure 36) shows its increase towards the north western corner of the field where it reaches the maximum value of 538 ft. at Syrah – 6Xst well. The growth thickness decreases towards the south eastern direction of the study area to reach its minimum value of 335 ft. at Syrah- 1X well.

Table 1: Summary of petrophysical results of Upper and Lower Safa reservoirs.

Well name	Gross (ft)	Pay (ft)	Vsh (%)	Ø	SW (%)
Upper Safa					
Syrah – 1X	335	3	10	11	10
Syrah – 5X	470	17	13	8.2	33
Syrah – 6Xst	538	16	12	9.1	23
Syrah – 8X	402	20	6	8.5	16
Lower Safa					
Syrah – 1X	766	158	5	10	8
Syrah – 5X	590	211	3	9	17
Syrah – 6Xst	668	244	8	10	16
Syrah – 8X	660	0	6	9	92

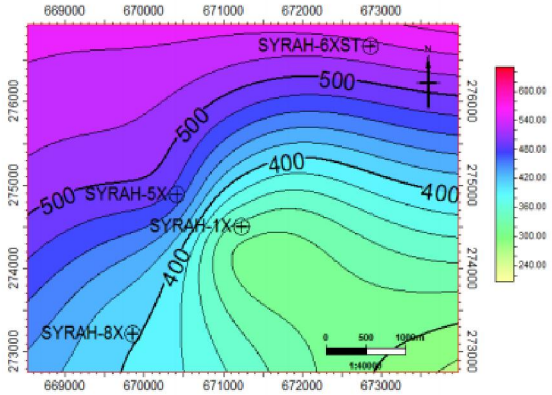

Figure 36: Gross map of Upper Safa reservoir, Syrah Field, North western Desert, Egypt

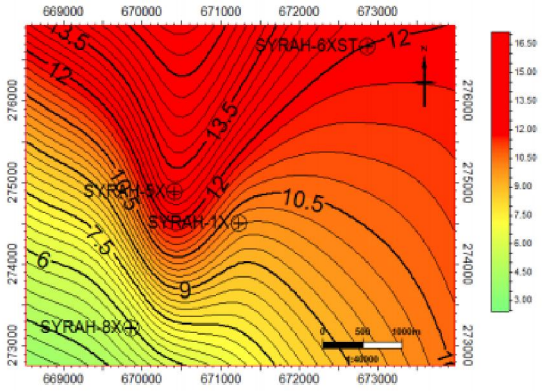

Figure 37: Shale volume map of Upper Safa reservoir, Syrah Field, North western Desert, Egypt

Figure (37) shows the shale volume distribution in Upper Safa reservoir. Generally, it increases toward the north and east directions, to reach the maximum value of 13 % at Syrah – 5X well and it decreases

towards the south western direction to reach its minimum value of 6 % in Syrah – 8X well.

The effective porosity in Upper Safa reservoir shows increases toward the east direction of Syrah field where it reaches 11 % as a maximum value at Syrah - 1X well and decreases toward the west and the southwestern directions reaching 8.5% as a minimum value at Syrah – 8X well (Figure 38).

The water saturation distribution map for Upper Safa reservoir in Syrah field (Figure 39) shows that it increases toward the north western part of the study area, where it reaches the maximum value of 33% in Syrah – 5X well and decreases toward the west direction to reach the minimum value of 10% at Syrah – 1X.

Figures (40 and 41) show net pay sand and Net sand to gross thickness respectively distribution for upper Safa in Syrah field. Generally, they increase toward the south western direction, to reach the maximum value of 20 ft and 5 % respectively at Syrah – 8X well and it decreases towards the center of the field to reach the minimum value of 20 ft and 5 % respectively in Syrah – 1X well.

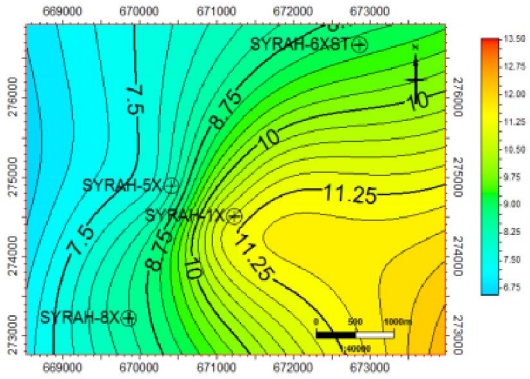

Figure 38: Effective Porosity map of Upper Safa reservoir, Syrah Field, North western Desert, Egypt.

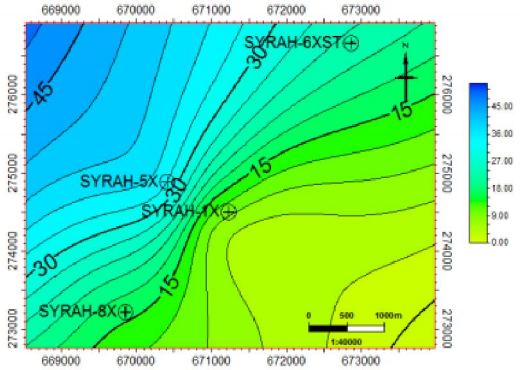

Figure 39: Water Saturation map of Upper Safa reservoir, Syrah Field, North western Desert, Egypt.

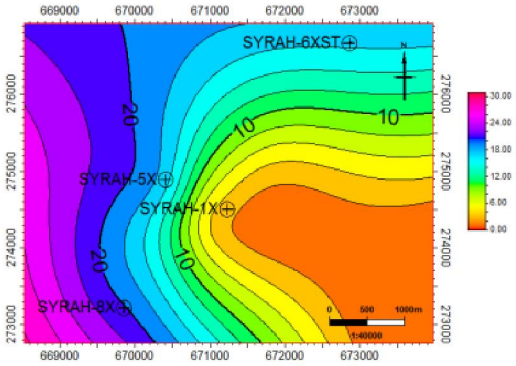

Figure 40: Net pay sand map of Upper Safa reservoir, Syrah Field, North western Desert, Egypt.

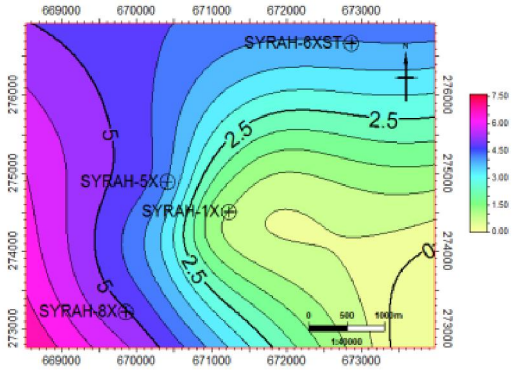

Figure 41: Net / Gross map of Upper Safa reservoir, Syrah Field, North western Desert, Egypt.

3.2.3.2 Lower Safa Reservoir maps

The total thickness distribution map for Lower Safa reservoir in Syrah field (Figure 42) shows that it increases towards the south eastern corner of the study area where, it reaches the maximum value of 766 ft. at Syrah – 1X well. The growth thickness decreases towards the north western direction of the study area to reach the minimum value of 590 ft. at Syrah- 5X well.

Figure (43) shows the shale volume distribution in Lower Safa reservoir. Generally, it increases toward the north direction to reach the maximum value of 8% at Syrah – 6Xst well and decreases towards the center of study area to reach the minimum value of 3 % in Syrah – 5X well.

The effective porosity in Lower Safa reservoir shows an increase toward the north eastern directions of Syrah field where it reaches 10.5% as a maximum value at Syrah - 6Xst well and decreases towards the south western direction to reach 9 % as a minimum value at Syrah – 8X well, as shown in Figure (44).

The water saturation distribution map for Lower Safa reservoir (Figure 45) shows that it increases toward the south western part of the study area, where it reaches the maximum value of 92% in Syrah – 8X well. The water saturation decreases toward the center

of study area to reach the minimum value of 8 % at Syrah – 1X.

Figures (46 and 47) show net pay sand and Net sand to gross thickness respectively distribution for the Lower Safa reservoir in Syrah field. Generally, they increases toward the north eastern direction, to reach the maximum value of 244 ft and 37 % respectively at Syrah – 6Xst well and decreases towards south western direction of the field to reach **the minimum value of 0 ft and 0 % respectively in** Syrah – 8X well.

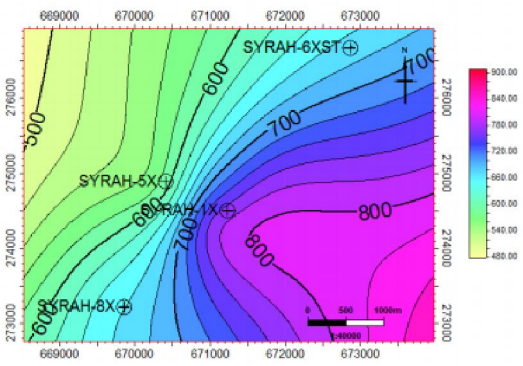

Figure 42: Gross map of Lower Safa reservoir, Syrah Field, North Western Desert, Egypt.

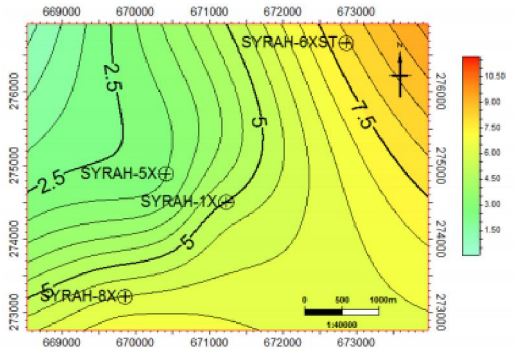

Figure 43: Shale volume map of Lower Safa reservoir, Syrah Field, North Western Desert, Egypt.

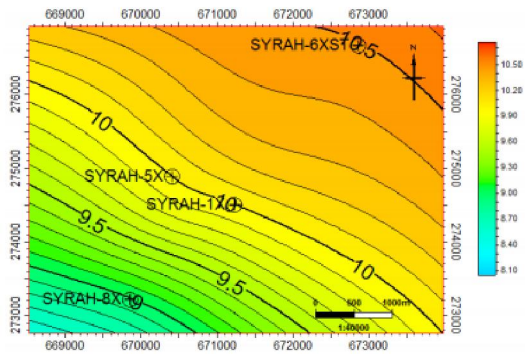

Figure 44: Effective Porosity map of Lower Safa reservoir, Syrah Field, North Western Desert, Egypt.

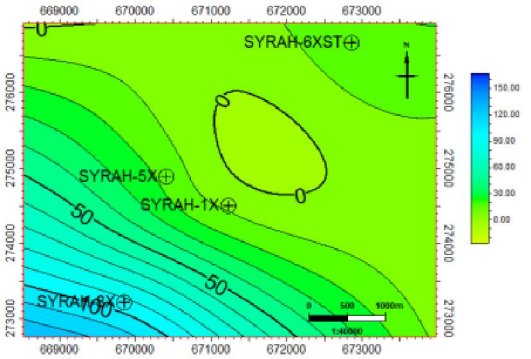

Figure 45: Water Saturation map of Lower Safa reservoir, Syrah Field, North Western Desert, Egypt.

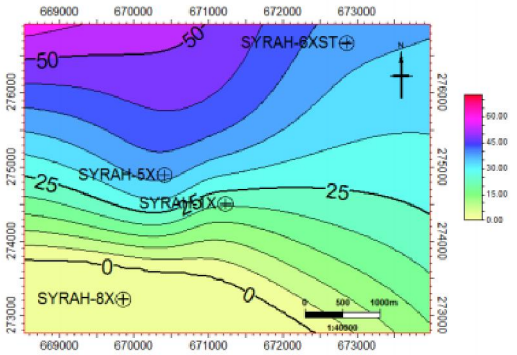

Figure 46: Net / Gross map of Lower Safa reservoir, Syrah Field, North Western Desert, Egypt.

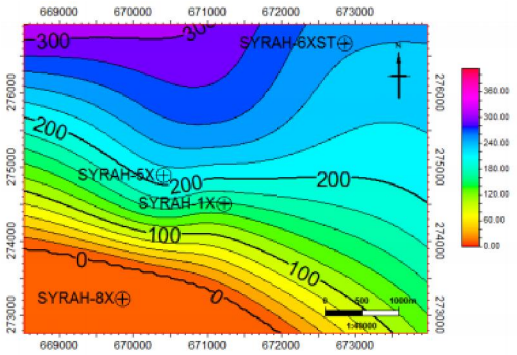

Figure 47: Net pay sand map of Lower Safa reservoir, Syrah Field, North Western Desert, Egypt.

4. Summary and Conclusions

Integration of petrographic description and open hole logs (gamma ray, density and neutron) enabled the construction of continuous accurate lithological column of the studied Safa Formation. Most of the section is composed of intercalations of clastic rocks except for some zones with metamorphic rocks that could not be identified directly from logs.

The use of spectral gamma ray log has significant improved the clay content evaluation, and therefore determination of the rock reservoir properties. In

extreme cases, the lack of this measurement may cause omission of a productive level.

Conventional analysis of petrophysical parameters from four wells distributed in Syrah field reveals the presence of four good quality reservoirs in the upper Safa member and three good quality reservoir in lower Safa member.

The reservoir pressure across lower Safa previewed water gradient range from 0.44 to 0.49 psi/ft in the lower body of sandstone. The upper body of sandstone, on the other hand, showed a connected gas gradient ranging from 0.1 to 0.11 psi/ft. Pressure values range from 6240 to 6280 psi in Syrah – 1X, Syrah – 5X and Syrah – 6Xst, indicating connectivity and 6950 psi in Syrah – 8X reflecting isolation in pressure.

Mapping of the petrophysical parameters of the Upper Safa reservoir showed that the total thickness increases towards the northwestern direction while the shale content increases toward the north and east directions. The effective porosity distribution indicates that porosity generally increases toward east. The hydrocarbon saturation increases toward the southeastern direction.

Mapping of the petrophysical parameters of Lower Safa reservoir showed that the total thickness increases towards the southeastern corner while the shale content increases toward north. The effective porosity distribution indicates that porosity generally increases toward the northeastern direction. The hydrocarbon saturation increases towards the northeastern direction.

References

1. Adams, J.A.S., and Weaver, C.E., 1958. Thorium-To-Uranium Ratios as Indicators of Sedimentary Processes: example of Concept of Geochemical Facies: American Association of Petroleum Geologists Bulletin, v. 42, p 387-430.
2. Archie, G. E., 1942. The Electrical resistivity log as an aid in determining some reservoir characteristics. 54 p.
3. Dolson, J.C., Shann, M. V., Matbouly, S., Harwood, C., Rashed, R. and Hammouda, H., 2001. The Petroleum Potential of Egypt, in W. A. Morgan. ed., Petroleum Provinces of the 21st Century, V. Memoir 74, Tulsa, Oklahoma, American Association of Petroleum Geologists, p 453-482.
4. Dott, R.H., 1964. Wacke, greywacke and matrix: what approach to immature sandstone classification, Journal of Sedimentary Petrology, v. 34, p 623 – 632.
5. El Awdan, F. Youssef, and A.R. Moustafa., 2002. Effect of Mesozoic and Tertiary Deformations on Hydrocarbon Exploration in the Northern Western Desert, Egypt". In Am. Assoc. Petrol. Geol. Int. Meeting, (Abstract).
6. Ellis, D., and Singer, J.M., 2008. Well Logging for Earth Scientists, 2nd edition. Springer, Dordrecht, 699 p.
7. El Shazly, E.M., 1977. The geology of the Egyptian region. In: A. E. M. Nair, W. H. Kanes & F. G. Stehli, The ocean basins and margins. Plenum press, V. 4 (A), p 379-444.
8. Fabricius, I.L., Fazladic, L.D., Steinholm, A., and Korsbech, U, 2003. The use of Spectral Natural Gamma Ray Analysis in Reservoir Evaluation of Siliciclastic Sediments: a Case Study from the Middle Jurassic of the Harald Field, Danish Central Graben: Geological Survey of Denmark and Greenland Bulletin, v. 1, p 349-366.
9. Fertl M.W, 2007. Gamma ray Spectral Logging: A new Evolution Frontier 2007. Part III – Measuring Source Rock Potential. World Oil, May 1983.
10. Hassan, M., Rossin, A., and Combaz, A., 1976. Fundamentals of the differential gamma ray log interpretation technique. 17th Ann. Log. Symp. SPWLA Trans., Paper H.
11. International Atomic Energy Agency (IAEA), 2003. Guidelines for Radioelement Mapping using Gamma Ray Spectrometry data, 179 p.
12. Khalda Petroleum Company Internal Report, 2014. Petrographic report for drill cutting samples from Syrah field, Western Desert, Egypt.
13. Hantar, G., 1990. North Western Desert. In: Said, R. (Eds.). The geology of Egypt. A. A. Balkema, Rotterdam, Netherlands. p 293–319.
14. Sultan, N., and Halim, M.A., 1988. Tectonic framework of northern Western Desert, Egypt and its effect on hydrocarbon accumulations. Proc. 9"' EGPC. Petrol. Explor. and Prod. Conf., 2, p 1-22.
15. Zein El Din, M. Y., Abd El-Gwad, E. A., El Shayb, H. M. and Haddad, I. A., 2001. Geological Studies and Hydrocarbons Potentialities of Mesozoic rocks in Ras Kanayis Onshore area, North Western Desert, Egypt. The Annals of the Geological Survey of Egypt, Vol. 12, p 325-337.

6/24/2018